Supplementary materials

Supplemental Figures:

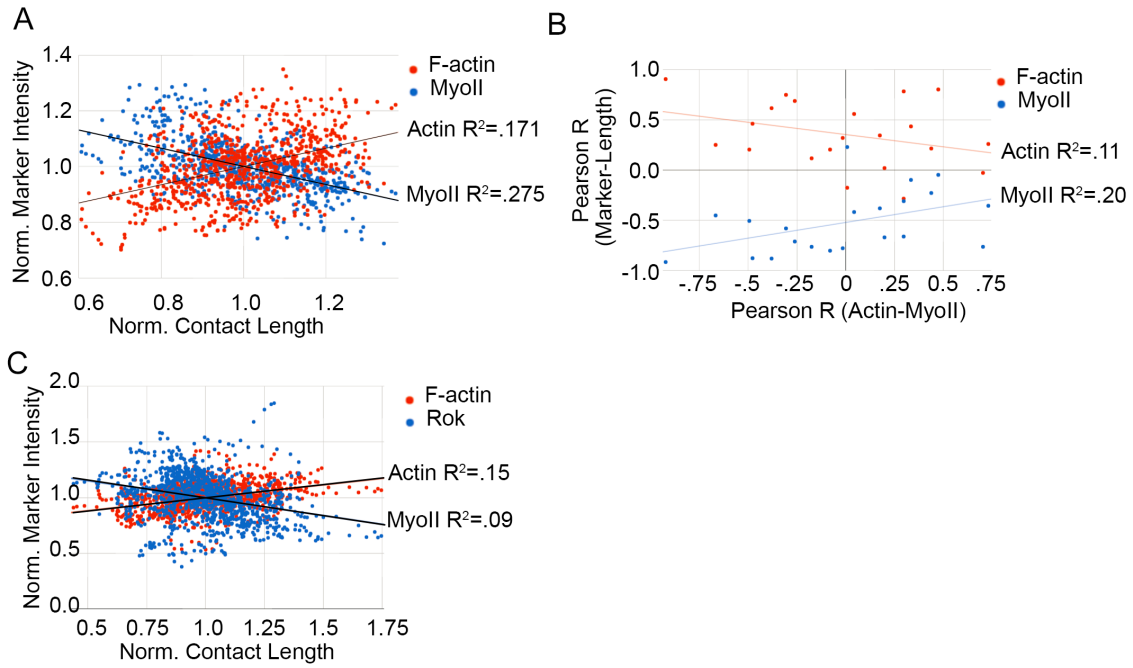

Figure S1: Related to Figure 1 and Figure 3. Cytoskeletal components correlate with contact length. (A) Scatterplot showing mean F-actin (red) and MyoII (blue) intensity plotted as a function of contact length. F-actin and MyoII exhibit positive and negative correlations with contact length, respectively. (B) Scatterplot of the Pearson R value at t=-1 between contact length and F-actin (red) or MyoII (blue) as a function of the F-actin-MyoII correlation. Each pair of vertical red and blue dots is from a single contact. Progressively stronger positive F-actin-contact length correlations or stronger MyoII-contact length correlations tend to have the strongest negative MyoII-F-actin cross-correlation. (C) Scatterplot showing mean F-actin (red) and Rok (blue) intensity plotted as a function of contact length. F-actin and Rok exhibit positive and negative correlations with contact length, respectively.

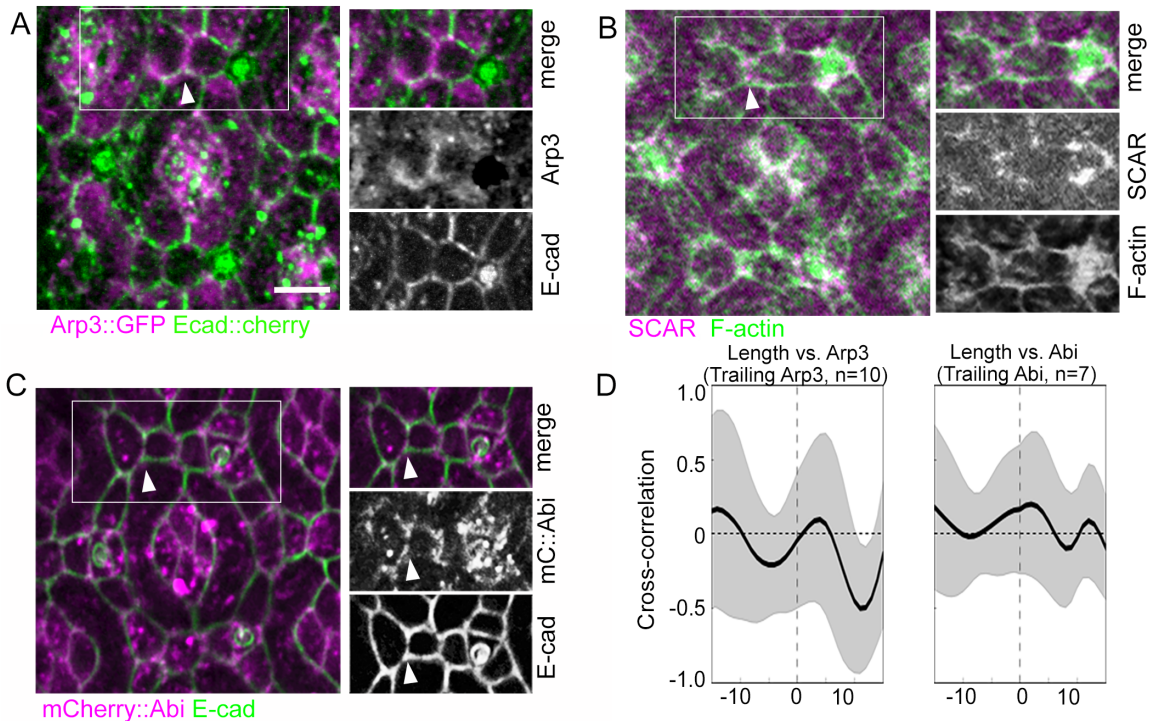

Figure S2: Related to Figure 3. Arp3, SCAR and Abi accumulate preferentially at the level of the adherens junctions along LC-LC contacts. (A) Arp3 tagged with GFP (Arp3::GFP). (B) Endogenous SCAR protein detected by immunofluorescence. (C) Abi protein tagged with mCherry (mCherry::Abi). The three regulators of protrusive F-actin branching accumulate at the level of the adherens junctions, marked with E-cad in A and C and with F-actin in B, and preferentially at LC-LC contacts. Arrowhead marks a representative LC-LC contact in each panel. Scale bar = 5 μm.

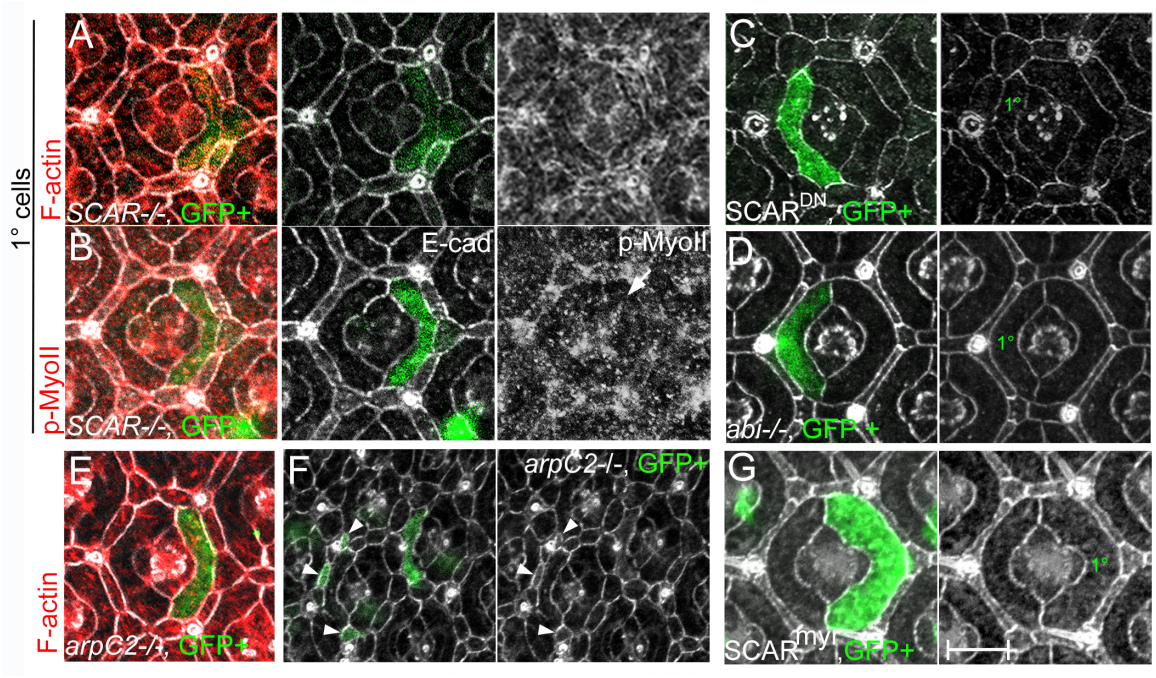

Figure S3: Related to Figure 3. The WRC and the Arp2/3 complex are required to promote the expansion of cells apical area and inhibit delamination of LCs. Eyes bearing GFP-positive (A-B) *SCAR* mutant cells, (C) SCAR dominant negative ($SCAR^{DN}$) expressing cell, (D) *abi* mutant cell, (E-F) *arpC2* mutant cells and (F) $SCAR^{myr}$ expressing cell. The apical area of the *SCAR*, *abi* and *arpC2* mutant cells as well as $SCAR^{DN}$ expressing cells is smaller compared to wild type (quantified in Fig. 3I) while the apical area of $SCAR^{myr}$ expressing cells is larger. Levels of (A) F-actin and (B) phospho-MyoII (p-MyoII) are comparable between *SCAR* mutant cells and wild type neighbors. (C, E) Mostly 1° *abi* and *arpC2* mutant cells were recovered at 42h APF. (F) However, inspection of eyes at earlier stages revealed abundant *arpC2* mutant LCs (marked by arrowheads) with reduced apical area that appeared to be delaminating from the epithelium implying that mutant LCs are preferentially eliminated from the lattice. Scale bar = 5 μm.

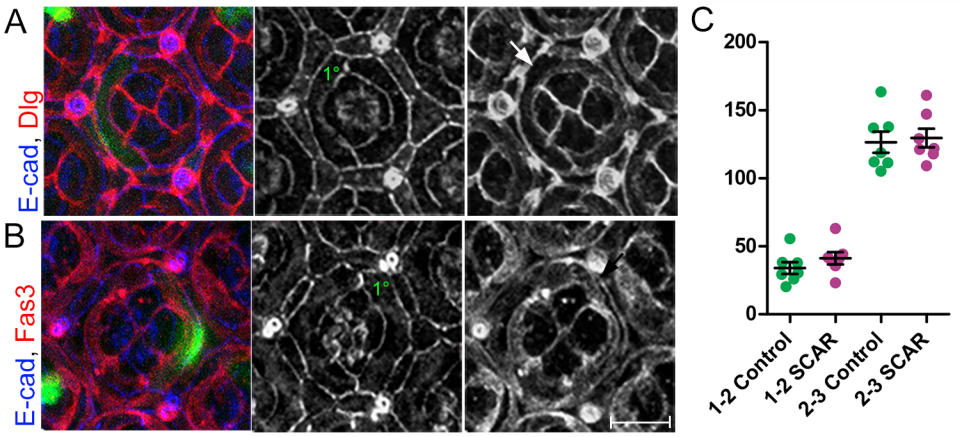

Figure S4: Related to Figure 3. Adherens juncions and septate junctions appear intact in *SCAR* mutant cells. The accumulation of (A) Fas3, (B) Dlg as well as (A-B) E-cad in *SCAR* mutant cells marked with GFP was comparable to adjacent wild type cells. (C) E-cad fluorescent intensity along 1°-2° and 2°-3° contacts in *SCAR* mutant cells (purple) compared to wild type (green) cells was unchanged. Scale bar = 5 μm.

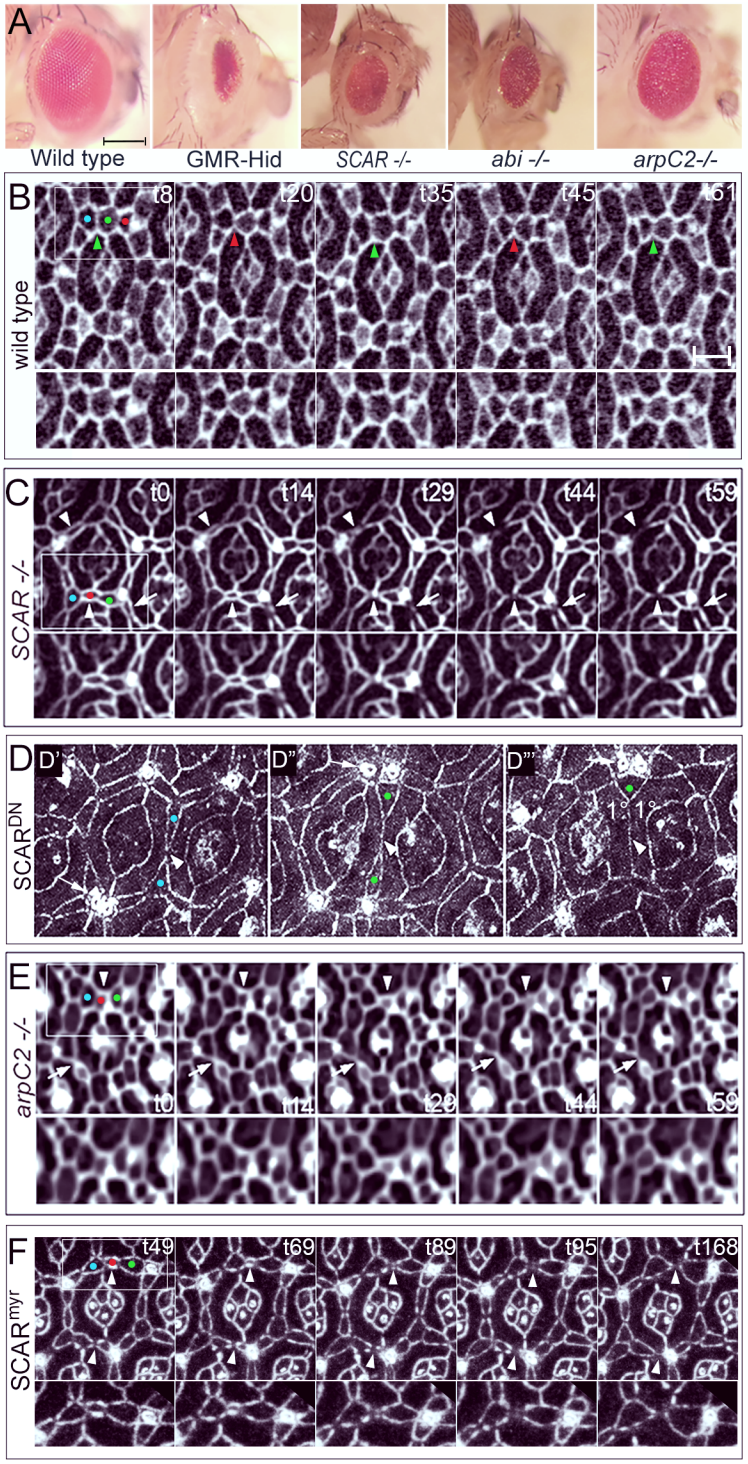

Figure S5: Related to Figure 4. *SCAR* and *arpC2* are required to maintain LC-LC contacts and reestablish LC-LC contacts following delamination of doomed LCs. (A) Phenotypes in adult eyes

and (B-F) cell behavior in eyes with impaired *SCAR, abi* or *arpC2* function compared to wild type (Movie 1 and movies not shown).

(A) Eyes composed entirely of *SCAR*, *abi* or *arpC2* mutant cells were rough and smaller then wild type. Wild type eyes form a regular crystalline surface. In GMR>Hid eyes most cells die by apoptosis. *SCAR*, *abi*, and *arpC2* mutant eyes generated by the rescue of the retina from Hid-mediated apoptosis using the EGUF technique were smaller compared to wild type and the regular crystalline arrangement of ommatidia was replaced with an irregular rough surface. Scale bar = 150 μm.

(B-F) Cell outlines were labeled with either E-cad::GFP or α–Cat::Venus. (B) Wild type eye. LC-LC contacts lengthen and shorten during lattice remodeling as the LCs change shape and cells delaminate from the lattice. (C) *SCAR* mutant eye. The LCs largely arranged in a single row. Following delamination of doomed LCs a subset of the LC-LC contacts fail to reestablish resulting in aberrant contacts between 1° cells of adjacent ommatidia (arrowheads), or in gaps in the contour of the AJs (arrows). Some of the gaps were repaired within several minutes. (D) Broad expression of a $SCAR^{DN}$ protein resulted in loss of LC-LC contacts. Arrowheads point to aberrant 1°-1° contacts, arrows to edges of the lattice that are missing resulting in clustering of bristles. (E) Similar defects were observed in *arpC2* mutant eyes. Arrow points to separating LC-LC contacts, arrowhead to a failure to reestablish LC-LC contacts following delamination of doomed LCs. (F) Broad expression of membrane tethered $SCAR^{myr}$ protein resulted in more constricted LC-LC contacts, gaps in the contour of the AJs at and near LC-LC contacts. In addition, a subset of the LC-LC contact failed to re-reestablish following delamination of doomed LCs resulting in aberrant contacts between 1° cell of neighboring ommatidia (examples marked with arrowheads). Scale bar = 5 μm.

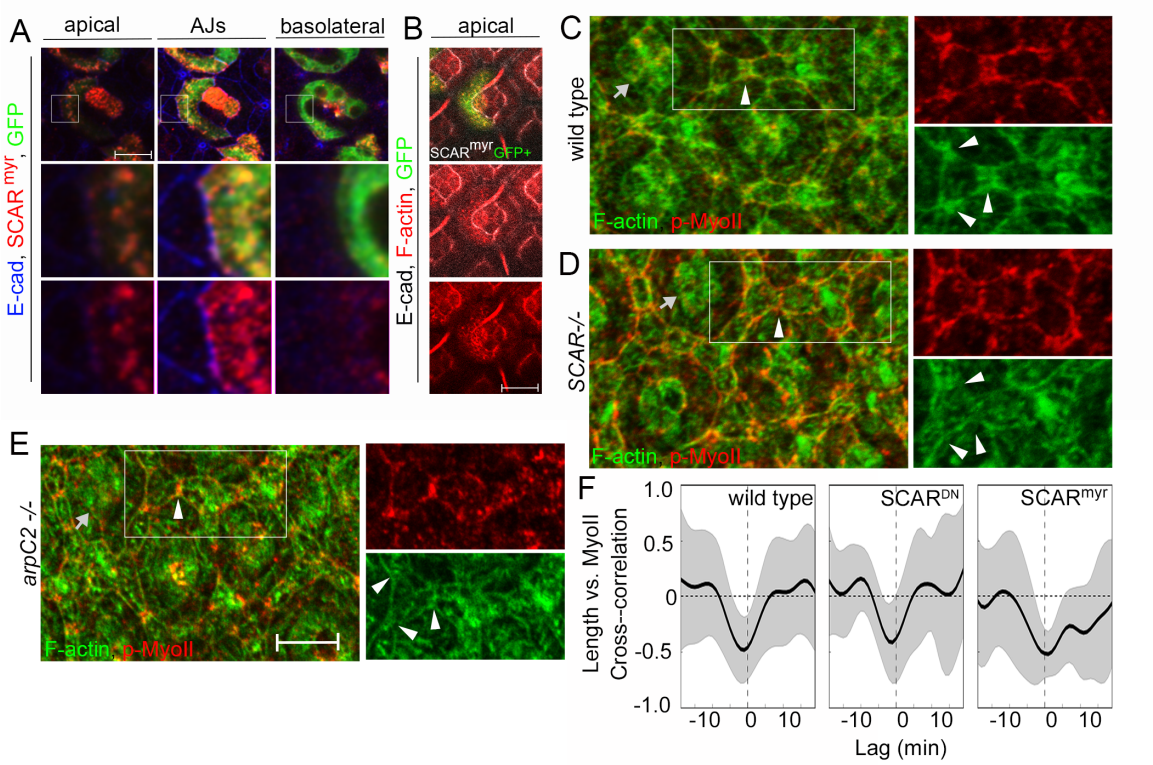

Figure S6: **Related to Figure 4. *SCAR* and *arpC2* influence F-actin organization.**

(A-B) SCAR^{myr} localizes broadly to the cells apical area and adherens junctions and promotes ectopic apical accumulation of F-actin. (A) Optical sections at the level of the apical surface (left row), the AJs (middle row) and the basolateral region (right row) in a SCAR^{myr} expressing cell marked with GFP. SCAR^{myr} accumulated broadly in the cells apical area and cell surface and in a close apposition to the cell surface at the level of the AJs, and was not detected in the basolateral region. The two bottom columns zoom on the boxed area in the top column. (B) F-actin accumulated ectopically and concentrated in foci at the apical surface in SCAR^{myr} expressing cells.

(C-E) F-actin and p-MyoII accumulation in wild type compared to *SCAR* and *arpC2* mutant eyes. (C) Wild type. F-actin and p-MyoII accumulate preferentially along LC-LC contacts (arrowheads in left panels point to a single representative LC-LC contacts; arrowheads in right panels point to F-

actin accumulation along LC-LC contacts). F-actin levels decreased along LC-LC contacts, while p-MyoII remained localized to the LC-LC contacts in both (D) *SCAR* and (E) *arpC2* mutant eyes. F-actin levels also decreased along cone-cone contacts in *SCAR* and *arpC2* mutants compared to wild type (arrows in left panels).

(F) Pearson cross-correlations between MyoII intensity and contact length. Broad expression of $SCAR^{DN}$ or $SCAR^{Myr}$ did not alter the negative correlation between MyoII and contact length.

Scale bar in A-C = 5 μm